

# Ex vivo glycan engineering of CD44 programs human multipotent mesenchymal stromal cell trafficking to bone

Robert Sackstein<sup>1,2</sup>, Jasmine S Merzaban<sup>1</sup>, Derek W Cain<sup>1</sup>, Nilesh M Dagia<sup>1</sup>, Joel A Spencer<sup>3</sup>, Charles P Lin<sup>3</sup> & Roland Wohlgenuth<sup>4</sup>

**The capacity to direct migration ('homing') of blood-borne cells to a predetermined anatomic compartment is vital to stem cell-based tissue engineering and other adoptive cellular therapies. Although multipotent mesenchymal stromal cells (MSCs, also termed 'mesenchymal stem cells') hold the potential for curing generalized skeletal diseases, their clinical effectiveness is constrained by the poor osteotropism of infused MSCs (refs. 1–3). Cellular recruitment to bone occurs within specialized marrow vessels that constitutively express vascular E-selectin<sup>4,5</sup>, a lectin that recognizes sialofucosylated determinants on its various ligands. We show here that human MSCs do not express E-selectin ligands, but express a CD44 glycoform bearing  $\alpha$ -2,3-sialyl modifications. Using an  $\alpha$ -1,3-fucosyltransferase preparation and enzymatic conditions specifically designed for treating live cells, we converted the native CD44 glycoform on MSCs into hematopoietic cell E-selectin/L-selectin ligand (HCELL)<sup>6</sup>, which conferred potent E-selectin binding without effects on cell viability or multipotency. Real-time intravital microscopy in immunocompromised (NOD/SCID) mice showed that intravenously infused HCELL<sup>+</sup> MSCs infiltrated marrow within hours of infusion, with ensuing rare foci of endosteally localized cells and human osteoid generation. These findings establish that the HCELL glycoform of CD44 confers tropism to bone and unveil a readily translatable roadmap for programming cellular trafficking by chemical engineering of glycans on a distinct membrane glycoprotein.**

Generalized skeletal diseases, such as osteoporosis and osteogenesis imperfecta, are currently incurable and cause considerable morbidity and mortality. MSCs hold great promise for treating or curing congenital and acquired bone diseases, as well as for regeneration or recovery of non-osteoid tissues such as ischemic myocardium<sup>1,7–10</sup>. The first essential step in regenerative therapeutics is to ensure adequate delivery of pertinent cells to the requisite tissue(s). Primary clinical considerations dictate that the vascular route is the preferred mode of administration of the cells, especially for treatment of systemic skeletal diseases, but infused MSCs lack any significant

osteotropism. We therefore sought to determine whether human MSCs could be engineered to navigate to bone.

Cell migration involves a cascade of events initiated by shear-resistant adhesive interactions between flowing cells and the vascular endothelium at the target tissue (step 1)<sup>11</sup>. This process is mediated by 'homing receptors' expressed on circulating cells that engage relevant endothelial coreceptors, resulting in cell-tethering and rolling contacts on the endothelial surface; this is typically followed by chemokine-triggered activation of integrin adhesiveness (step 2), firm adhesion (step 3) and extravasation (step 4)<sup>11</sup>. The portal for cell migration into bone is the marrow, and *in vivo* studies have revealed a key role for vascular E-selectin (CD62E) in step 1 of this process<sup>4</sup>. Although E-selectin expression is typically induced by inflammation, it is present constitutively on marrow microvasculature<sup>4,5</sup>, where it co-localizes with the chemokine CXCL12 (SDF-1) uniquely within endothelial beds that are sites of cellular recruitment<sup>4</sup>.

Like the other Ca<sup>2+</sup>-dependent lectins comprising the selectin family, L-selectin (CD62L) and P-selectin (CD62P), E-selectin binds specialized carbohydrate determinants, prototypically consisting of sialofucosylations containing an  $\alpha$ -2,3-linked sialic acid substitution on galactose and an  $\alpha$ -1,3-linked fucose modification on N-acetylglucosamine, that are together displayed as the terminal tetrasaccharide sialyl Lewis X (sLe<sup>x</sup>, NeuAc $\alpha$ 2-3Gal $\beta$ 1-4[Fuc $\alpha$ 1-3]GlcNAc $\beta$ 1-R)<sup>11,12</sup>. Hematopoietic stem/progenitor cells (HSPCs) express E-selectin ligands and CXCR4 (the receptor for CXCL12), which are crucial for directing HSPC homing to bone<sup>13</sup>. Two principal ligands for E-selectin are found on HSPCs: P-selectin glycoprotein ligand-1 (PSGL-1) and a sialofucosylated glycoform of the CD44 protein known as HCELL (refs. 6,14). CD44 is a rather ubiquitous cell membrane protein, but the HCELL glycoform is natively expressed exclusively on human HSPCs. HCELL is functionally defined as a form of CD44 having binding activity to E-selectin, L-selectin or both under hemodynamic shear conditions, and it can be identified in western blots of cell lysates as a CD44 glycoform reactive with an E-selectin-immunoglobulin chimera (E-Ig) and with the monoclonal antibody (mAb) HECA452, which recognizes an sLe<sup>x</sup>-like epitope. On human HSPCs, HCELL is the most potent E- and L-selectin ligand, and it displays relevant  $\alpha$ -2,3-sialic acid and  $\alpha$ -1,3-fucose binding

<sup>1</sup>Departments of Dermatology and Medicine, Brigham and Women's Hospital and Harvard Skin Disease Research Center, <sup>2</sup>Department of Medical Oncology, Dana-Farber Cancer Institute and <sup>3</sup>Wellman Center for Photomedicine, Massachusetts General Hospital, Harvard Medical School, Boston, Massachusetts 02115, USA. <sup>4</sup>Research Specialties, Sigma-Aldrich, Buchs CH-9470, Switzerland. Correspondence should be addressed to R.S. (rsackstein@rics.bwh.harvard.edu).

Received 22 October 2007; accepted 5 December 2007; published online 13 January 2008; doi:10.1038/nm1703

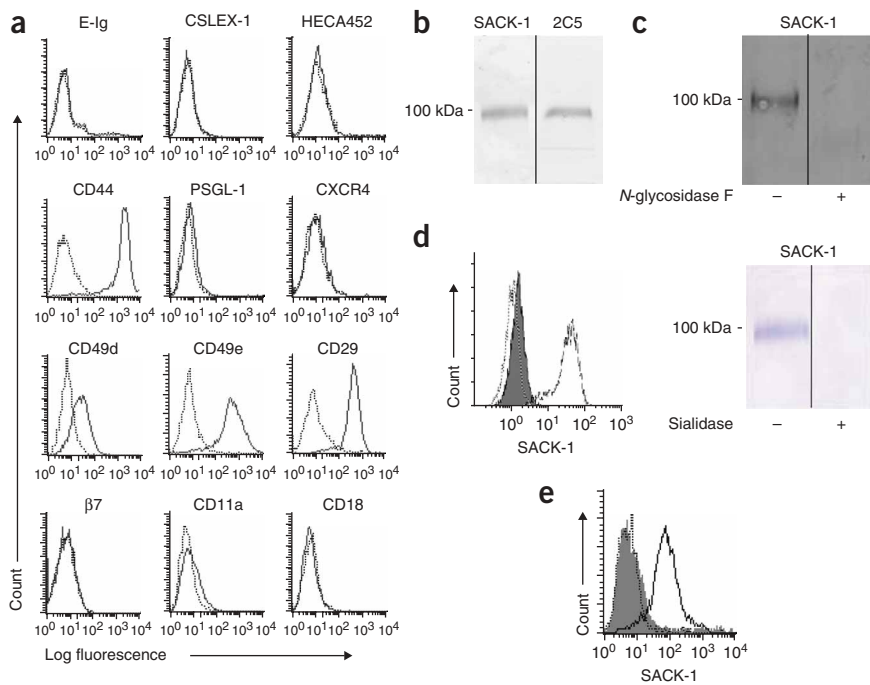


**Figure 1** MSCs lack E-selectin ligands but express CD44 reactive with SACK-1 mAb, which recognizes a sialic acid–dependent epitope displayed on a CD44-specific *N*-glycan substitution. **(a)** Flow cytometric analysis of E-selectin ligand activity (E-Ig binding) and of HECA452, CSLEX1, CD44, PSGL-1, CXCR4, CD49d/CD29 (VLA-4), CD49e/CD29 (VLA-5), CD49d/β7 (LPAM-1) and CD11a/CD18 (LFA-1) expression on MSCs. Dotted line is isotype control, black line is specific antibody (or E-Ig chimera). **(b)** Western blot analysis of whole cell lysates of KG1a cells showing SACK-1 staining (left) of a single glycoprotein of ~100 kDa with mobility identical to that stained by 2C5 mAb to CD44 (right). **(c)** SACK-1 staining of western blots of untreated (–) or *N*-glycosidase F–treated (+) immunoprecipitated CD44 from KG1a cells. **(d)** Left, flow cytometric analysis of isotype control (dotted line) and SACK-1 expression on untreated (black line) and α-2,3-sialidase–treated (shaded) KG1a cells. Right, SACK-1 staining of western blots of untreated (–) or sialidase-treated (+) immunoprecipitated CD44 from KG1a cells. **(e)** Flow cytometric analysis of SACK-1 expression on MSCs. Dotted line is isotype control, black line is SACK-1, and the shaded histogram denotes SACK-1 reactivity after sialidase treatment of MSCs. All results shown are representative of flow cytometry experiments performed on each MSC culture derived from  $n = 17$  marrow donors and of western blots of lysates from each of these cultures.

determinants on *N*-glycans<sup>6,14,15</sup>. Aside from E-selectin ligands and CXCR4, HSPCs express several integrins that are also pivotal in trafficking to bone, including VLA-4 (also known as α<sub>4</sub>β<sub>1</sub> or CD49d/CD29), VLA-5 (α<sub>5</sub>β<sub>1</sub> or CD49e/CD29), LPAM-1 (α<sub>4</sub>β<sub>7</sub>) and LFA-1 (α<sub>1</sub>β<sub>2</sub> or CD11a/CD18)<sup>13</sup>. Engagement of CXCR4 on HSPCs (via CXCL12 binding) activates HSPC integrins to bind their respective endothelial ligands, but E-selectin receptor–ligand interactions are not influenced by chemokines.

In contrast to abundant data regarding HSPC osteotropism, the molecular basis of MSC trafficking to bone has not been well studied. To address this issue, we analyzed the expression of characterized HSPC homing molecules on MSCs cultured according to an established protocol<sup>16</sup> from normal human marrow ( $n = 17$  donors). The MSCs showed surface markers characteristic of these cell types (absence of CD34 and CD45 and presence of CD73, CD90 and CD105; see **Supplementary Fig. 1** online), and were capable of multipotent differentiation *in vitro* toward cells with osteoblast, adipocyte and fibroblast phenotypes as previously described<sup>16</sup>. As determined by flow cytometry, all MSCs were devoid of reactivity with E-Ig, indicating the absence of E-selectin ligands (**Fig. 1a**); they did not stain with mAb CSLEX1 or HECA452 (each of which identifies

sLe<sup>x</sup>) and did not express PSGL-1 (**Fig. 1a**). MSCs also lacked both chains of LFA-1 and the β<sub>7</sub> chain of LPAM-1, but expressed the other α<sub>4</sub> integrin, VLA-4, and also expressed VLA-5 (**Fig. 1a**). Notably, flow cytometry of suspended cells and immunofluorescence studies of plate-adherent MSCs (*in situ*, without trypsinization) showed no expression of CXCR4 (**Fig. 1a**), and MSCs did not migrate in response to CXCL12 in either static or flow-based assays (data not shown). These data show that MSCs lack many effectors of homing to bone, especially E-selectin ligands and CXCR4, thus prompting us to analyze whether programming the expression of such molecules in these cells could allow for osteotropism.

As previously reported<sup>9,16</sup>, CD44 was strongly expressed by cultured MSCs (**Fig. 1a**). Thus, the absence of HCELL expression is due not to deficiency of CD44 but rather to the lack of pertinent carbohydrate decorations, such as glycans modified with α-2,3-sialic acid, α-1,3-fucose or both. To provide further insight into CD44 glycans, we tested whether MSCs react with SACK-1, a mAb generated against HCELL isolated from the human myeloid leukemia cell line KG1a (refs. 6,14,15). SACK-1 is a CD44-specific mAb (**Fig. 1b**) that identifies an α-2,3-sialylated epitope expressed exclusively on *N*-glycan modifications of CD44, as binding is eliminated after digestion with *N*-glycosidase F (**Fig. 1c**) or after digestion with an α-2,3-specific sialidase from *Streptococcus pneumoniae* (**Fig. 1d**).

Conspicuously, SACK-1 reactivity was high on all MSCs from all donors and, appropriately, sensitive to sialidase digestion (**Fig. 1e**). These data indicated that MSCs

express CD44 possessing α-2,3-sialylated *N*-glycans, suggesting that the absence of HCELL expression could reflect a relative paucity of α-1,3-fucose modifications. We thus reasoned that stereoselective addition of fucose residues to membrane CD44 would yield HCELL. To test this hypothesis, we used an α-1,3 linkage–specific fucosyltransferase, fucosyltransferase VI (FTVI). In the presence of donor fucose substrate (GDP-fucose), this glycosyltransferase places fucose in α-1,3 linkage to an acceptor *N*-acetylglucosamine located specifically within a terminal type 2 lactosamine unit (Galβ1–4GlcNAcβ1–R); if the lactosamine is α-2,3-sialylated, the sLe<sup>x</sup> determinant is created.

For custom engineering of cell surface glycans, it is essential that target cells remain viable and retain the requisite native phenotype after manipulation. The development of glycosyltransferases has been inspired heretofore by the desire to glycan-modify soluble organic molecules biocatalytically (for example, glycoproteins for pharmacologic purposes), as the use of enzymes to add relevant glycans in appropriate linkage(s) is more efficient and precise than traditional organic synthesis, which requires cumbersome protection–deprotection loops. Hence, the cell toxicities inherent to glycosyltransferases and their attendant buffer conditions have been overlooked in the development of these reagents and were not appreciated in prior studies

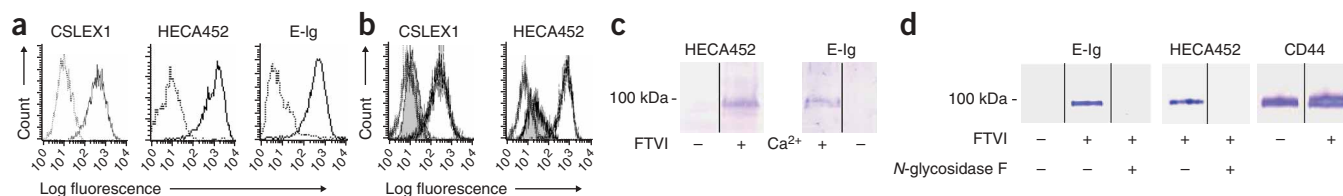


**Figure 2** FTVI treatment of MSCs elaborates sialofucosylations on *N*-linked glycans of CD44, resulting in HCELL expression. **(a)** Flow cytometric analysis of CSLEX1, HECA452 and E-Ig reactivity on untreated and FTVI-treated MSCs. Dotted line is untreated MSCs and black line is FTVI-treated MSCs. **(b)** Flow cytometric analysis of CSLEX1 and HECA452 reactivity of FTVI-treated MSCs undigested (solid line) or digested with proteinase K (shaded histogram) before FTVI treatment; dotted line is isotype control staining. **(c)** Western blot analysis of HECA452 (left) and E-Ig (right) reactivity of MSC lysates. Staining of FTVI-treated MSCs with E-Ig was performed in the presence (+) or absence (-) of  $\text{Ca}^{2+}$ . FTVI treatment induced HECA452-reactive sialofucosylations and E-Ig binding selectively on a ~100-kDa glycoprotein. **(d)** CD44 was immunoprecipitated (with Hermes-1 mAb to CD44) from equivalent amounts of cell lysates from FTVI-treated (+) or untreated (-) MSCs, and immunoprecipitates were digested with *N*-glycosidase F (+) or treated with buffer (-). Immunoprecipitates were then electrophoresed and blotted with HECA452, E-Ig or 2C5. Results are representative of experiments performed on each MSC culture derived from  $n = 17$  marrow donors.

using this technology on live cells<sup>17–19</sup>. Indeed, when we used the commercial FTVI preparation and reaction conditions used by others<sup>17–19</sup>, we found that >95% of MSCs died within 8 h of fucosylation. We determined that the cytotoxicity resulted from exposure to stabilizers (for example, glycerol) in the enzyme formulation and exposure to the high concentrations of  $\text{Mn}^{2+}$  (10 mM) used in the enzymatic reaction, a catalyst hitherto deemed essential for high-efficiency fucosyltransferase activity<sup>20</sup>. Consistent with prior reports<sup>21</sup>, we observed that 10 mM  $\text{Mn}^{2+}$  alone induced prominent cell death in MSCs (as well as in HSPCs) evident several hours after exposure ( $\text{Mn}^{2+}$ -induced death was uniformly >90% at 8 h; **Supplementary Fig. 2** online). Aside from cytotoxicity,  $\text{Mn}^{2+}$  triggers signal transduction<sup>22</sup> and stimulates integrin adhesiveness (for example, for VLA-4, VLA-5 and LFA-1) in human hematopoietic cells at concentrations far below those used in forced fucosylation ( $\leq 1$  mM)<sup>23,24</sup> and with an activation potency exceeding that of the chemokine CXCL12 (refs. 23–25). Thus,  $\text{Mn}^{2+}$ -induced upregulation of integrin-mediated adhesion itself would profoundly affect cell trafficking, confounding the effect(s) of  $\alpha$ -1,3-fucosylation. To address these problems, we developed a new method for high-titer FTVI production followed by enzyme stabilization in buffer chosen specifically for cell compatibility (HBSS), and we deliberately optimized the FTVI coupling reaction in the absence of any divalent cations, thus avoiding cytotoxicity and integrin activation. These new conditions resulted in high-efficiency  $\alpha$ -1,3-fucosylation of CD44 with 100% cell viability.

After enforced  $\alpha$ -1,3-fucosylation, all cultured MSCs stained with mAbs CSLEX1 and HECA452, consistent with strong expression of sLe<sup>x</sup> epitopes (**Fig. 2a**) with concomitant prominent binding of E-Ig (**Fig. 2a**) but not P-selectin-immunoglobulin chimera (**Supplementary Fig. 3** online). There were no changes in other cell membrane markers analyzed (as in **Fig. 1a**), nor were there any effects on VLA-4 or VLA-5 binding to pertinent fibronectin fragments (data not shown). Proteinase K digestion of MSCs before FTVI treatment markedly diminished CSLEX1 and HECA452 reactivity (mean channel fluorescence consistently <10% of that for undigested cells; see **Fig. 2b**), indicating that the sialofucosylated determinants were created principally on membrane glycoproteins, not glycolipids. Western blot analysis of cell lysates and of immunoprecipitated CD44 from FTVI-treated MSCs revealed that the only glycoprotein bearing the requisite sialofucosylations recognized by HECA452 was ‘standard’ (non-alternatively spliced) CD44 (~100 kDa; **Fig. 2c,d**) and the only glycoprotein supporting  $\text{Ca}^{2+}$ -dependent E-Ig binding was CD44 (**Fig. 2a,c,d**). As predicted by SACK-1 reactivity, the relevant sialofucosylations of CD44 were

displayed on *N*-glycans, as shown by abrogation of E-Ig binding after digestion with *N*-glycosidase F (**Fig. 2d**). Therefore,  $\alpha$ -1,3-fucosylation of MSCs generated HCELL.

To analyze the E-selectin–ligand activity of  $\alpha$ -1,3-fucosylated-MSCs under physiologic blood flow conditions, parallel-plate flow chamber studies were performed with human umbilical vein endothelial cells (HUVECs) stimulated by cytokines to express E-selectin. HCELL<sup>+</sup> MSCs showed marked E-selectin ligand activity that was completely abrogated in the presence of EDTA or by treatment of HCELL<sup>+</sup> MSCs with sialidase (**Fig. 3**). Prominent shear-resistant rolling interactions were observed at the usual postcapillary venular shear levels (1–4 dyn/cm<sup>2</sup>) persisting at upwards of 20 dyn/cm<sup>2</sup>, well outside the range in which PSGL-1 supports E-selectin binding<sup>6</sup>. These data indicate that engineered HCELL is a highly efficient effector of step 1 interactions, with properties similar to those of native HCELL displayed on KG1a

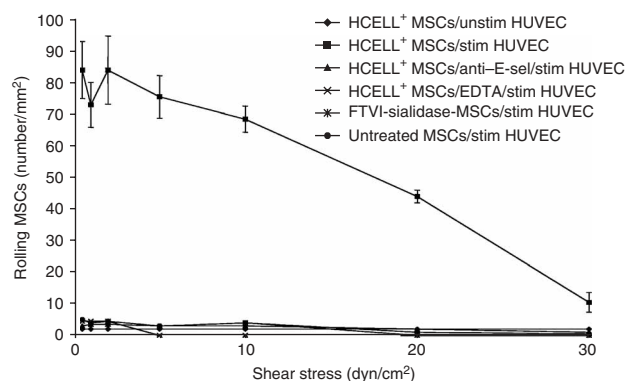


**Figure 3** HCELL<sup>+</sup> MSCs have markedly enhanced shear-resistant adhesive interactions with endothelial E-selectin under defined shear stress conditions. Untreated MSCs, HCELL<sup>+</sup> MSCs or sialidase-digested FTVI-treated (FTVI-sialidase-MSCs) MSCs were perfused over IL-1 $\beta$  and TNF- $\alpha$  stimulated (stim) or unstimulated (unstim) HUVECs at 0.5 dyn/cm<sup>2</sup>. MSC accumulation was then determined at shear stresses of 0.5, 1, 2, 5, 10, 20 and 30 dyn/cm<sup>2</sup>. HCELL<sup>+</sup> MSCs show rolling adhesive interactions on HUVECs at a shear stress of up to 30 dyn/cm<sup>2</sup> that were abrogated by sialidase treatment. To control for the specificity of binding of HCELL<sup>+</sup> MSCs, EDTA was added to the assay buffer (EDTA group), or stimulated HUVECs were pretreated with a function blocking mAb to E-selectin (anti-E-Sel group) before use in adhesion assays. Values are means  $\pm$  s.e.m. ( $n = 4$  for each group).  $P < 0.001$  for comparisons of HCELL<sup>+</sup> MSCs to all other groups at all shear stress levels.

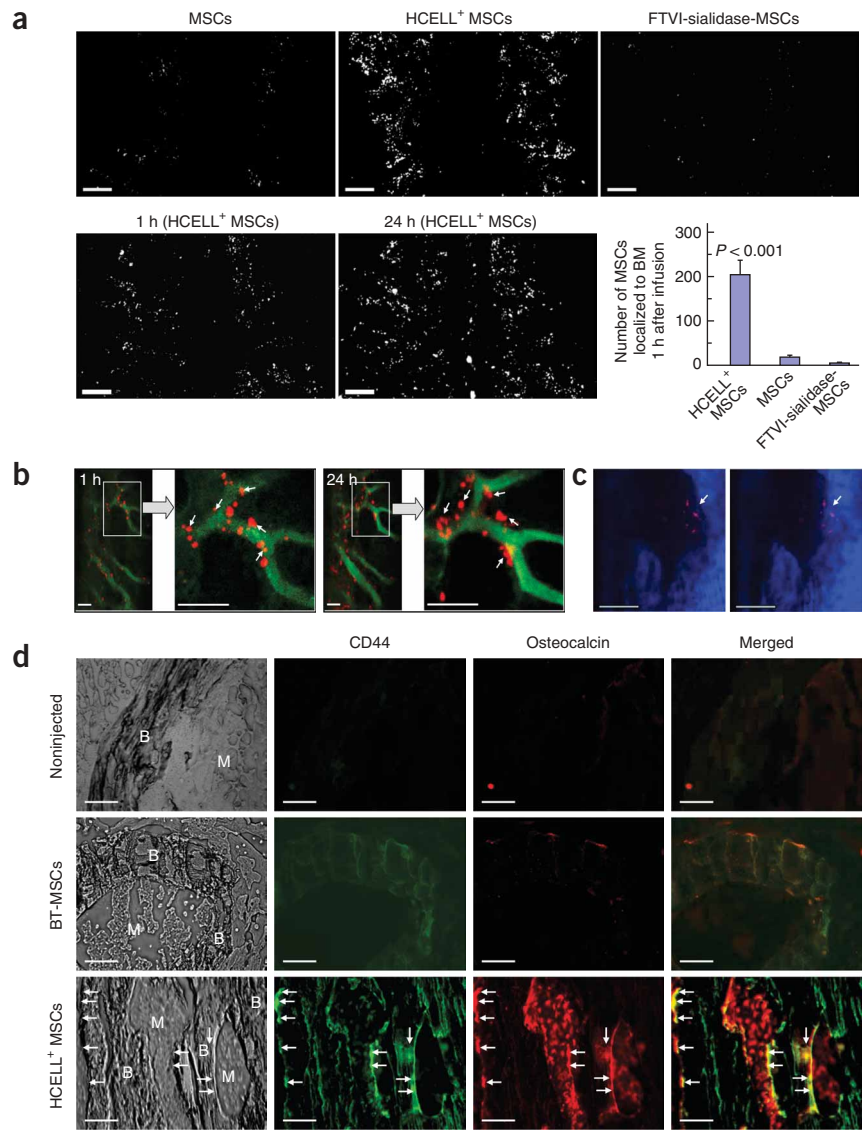
**Figure 4** Human MSC homing to mouse bone marrow. **(a)** Images obtained from intravital confocal microscopy of the parasagittal region of the calvarium in representative NOD/SCID mice at 1 h after infusion of the indicated cells (top). Results shown in the lower panels are representative images of one mouse at 1 h (left) and 24 h (right) after infusion of HCELL<sup>+</sup> MSCs. Scale bar, 250  $\mu$ m. Bar graph represents the number of MSCs localized to the bone marrow 1 h after infusion, mean  $\pm$  s.e.m. for  $n = 5$  experiments.  $P < 0.001$  for comparison of HCELL<sup>+</sup> MSCs to each other group. The middle bar in the graph ("MSCs") combines data from untreated MSCs and BT-MSCs, for which the results were identical.

**(b,c)** *In vivo* confocal and two-photon microscopy showing extravasation of human HCELL<sup>+</sup> MSCs in mouse marrow and subsequent migration to the endosteal surface after adoptive transfer; images are representative of  $n = 12$  experiments.

**(b)** DiD-labeled MSCs (red) primarily line the vessel walls (visualized by Angiosense 750, green) 1 h after transfer (left); at 24 h (right), MSCs have extravasated. The two images were obtained at the same site with the identical tissue plane. White boxes correspond to higher-magnification images. Most MSCs are intravascular at 1 h (arrows), but by 24 h, cells have infiltrated the marrow parenchyma (arrows).

**(c)** Second harmonic-generation imaging microscopy reveals close juxtaposition between DiD-labeled cells (red) and bone (collagen, blue) after 9 d. Bone image at right is 10  $\mu$ m above the image at left, showing the close proximity of the endosteum to the cells (arrows). Scale bar, 100  $\mu$ m.

**(d)** Immunofluorescence images of frozen calvarium sections from NOD/SCID mice that received intravenous injections of HCELL<sup>+</sup> MSCs or BT-MSCs as indicated ( $5 \times 10^6$  cells per mouse). The leftmost image in each row is a phase light microscopy image of the bone section. Twelve weeks after transplantation, the mice were killed and their skulls isolated, snap frozen and sectioned. Images are representative of  $n = 3$  separate experiments (with duplicate mice in each group for each experiment). Locations of bone and of bone marrow are designated by B and M, respectively; scale bars, 50  $\mu$ m. Sections were stained for human CD44 (green) and human osteocalcin (red); in the merged image, arrows indicate cells staining for CD44 in the vicinity of osteocalcin deposits (yellow). Specificity of mAb to human osteocalcin was confirmed by staining MSC before and after osteogenic differentiation *in vitro* (see **Supplementary Fig. 6** online).



cells and human HSPCs<sup>6,14</sup>. Enforced HCELL expression was stable for 24 h, subsequently declining to undetectable expression by 96 h, presumably owing to turnover of surface protein, as no changes in membrane CD44 levels were observed by flow cytometry (data not shown). MSC viability was unaffected by HCELL expression, and, in comparing untreated, buffer-treated and HCELL<sup>+</sup> MSCs, we found there were no differences in the number or proliferation of clones or in their differentiation into osteoblast or adipocyte lineages in clonogenic assays (>95% of clones showed differentiation to either lineage). Thus, enforced HCELL expression endows E-selectin binding without discernible untoward effects on the MSC phenotype *in vitro*.

To evaluate the effect of engineered HCELL expression on the homing of MSCs to bone *in vivo*, we used dynamic real-time confocal microscopy to visualize marrow sinusoidal vessels in the calvarium of live, immunodeficient (NOD/SCID) mouse hosts<sup>4</sup>. MSCs were labeled with tracer dye before injection into the tail veins of the host mice, and

four cell groups were evaluated: FTVI-treated MSCs (HCELL<sup>+</sup> MSCs), FTVI-treated MSCs digested with sialidase (FTVI-sialidase-MSCs), buffer-treated MSCs (BT-MSCs) and untreated MSCs. *In vivo* microscopy studies showed robust tethering and rolling interactions and firm adherence of HCELL<sup>+</sup> MSCs on sinusoidal vessels, and HCELL<sup>+</sup> MSCs infiltrated the marrow parenchyma rapidly, within hours of infusion (**Fig. 4a** and **Supplementary Video 1** online). In contrast, untreated MSCs and BT-MSCs showed minimal endothelial binding interactions and only modest infiltrates, whereas FTVI-sialidase-MSCs typically showed even lower levels of endothelial interactions and marrow infiltrates (**Fig. 4a** and **Supplementary Video 2** online). These results show that MSCs become osteotropic after FTVI treatment and further indicate that this osteotropism was not a result of  $\alpha$ -1,3-fucosylation *per se* or of indirect effects on other adhesion molecules (for example, VLA-4), but is instead a consequence of the induced HCELL E-selectin ligand activity, requiring concomitant expression

of  $\alpha$ -2,3-sialic acid and  $\alpha$ -1,3-fucose modifications. Of note, immunofluorescence microscopy of lung sections from mice killed at 1 and 24 h after injection showed substantial accumulations of MSCs in pulmonary microvessels no different from the other test groups, presumably a reflection of nonspecific 'steric trapping' (data not shown). However, infiltration of MSCs into marrow parenchyma was evident only in mice receiving HCELL<sup>+</sup> MSCs, as observed by simultaneous staining of MSCs and blood vessels (Fig. 4b). Compared to those seen in prior studies of HSPCs, these marrow infiltrates are noteworthy in that they occurred without manipulations of the mice that markedly enhance trafficking to marrow (for example, splenectomy)<sup>19</sup> or that induce sinusoidal injury, such as radiation<sup>18</sup>, which notably upregulate endothelial ligands mediating marrow homing<sup>26</sup>. Moreover, unlike HSPCs, the MSCs used here did not bear LFA-1, LPAM-1 or CXCR4 and did not undergo chemotaxis to CXCL12 (ref. 4); hence these molecules are not compulsory for the trafficking of MSCs to bone. Collectively, these data show that enforced expression of HCELL endows cells with the ability to navigate to bone and distinguish this CD44 glycoform as a bone-homing receptor.

To determine whether marrow-infiltrating HCELL<sup>+</sup> MSCs were localized to endosteal surfaces, we used intravital two-photon microscopy and immunofluorescence microscopy of frozen sections of mouse calvarium. Second harmonic-generation imaging of intravital two-photon optical sections<sup>27</sup> revealed focal areas of human MSCs apposed to mouse bone endosteum within 10 d of injection (Fig. 4c). Twelve weeks after injection, mouse calvarial bone was harvested and dual-color immunofluorescence staining for human CD44 and the bone-specific protein osteocalcin<sup>28</sup> was performed, together with Hoechst 33342 dye staining to identify cells. Sections of bone from mice that received untreated MSCs and BT-MSCs completely lacked staining by both mAb to human CD44 and mAb to human osteocalcin. However, bone sections of all mice ( $n = 6$ ) that received HCELL<sup>+</sup> MSCs showed foci of human CD44<sup>+</sup> cells colocalizing with human osteocalcin deposits (Fig. 4d; Hoechst 33342 staining shown in **Supplementary Fig. 4** online). These islands of human osteoid tissue were sparse, comprising <0.1% of bone area surveyed, but their presence in all mice receiving HCELL<sup>+</sup> MSCs indicates that marrow-infiltrating human MSCs retain the capacity to differentiate into osteoid elements within the mouse bone milieu. The observed scarcity of human osteoid tissue in normal adult mouse bone may result from an inhospitable environment for human bone formation, the slow turnover of native bone elements under steady-state conditions, the requirement for seeding of appropriate osteogenic niches or some combination of these factors. Although these results leave unanswered questions about the properties and efficiency of human bone formation in a xenogeneic environment, these data provide direct evidence that extravasated human HCELL<sup>+</sup> MSCs can seed endosteum and undergo osteogenic differentiation *in vivo*.

Our strategy for programming HCELL expression on MSCs consists of several steps (summarized in **Supplementary Fig. 5** online) that should serve as general guiding principles for future efforts in custom engineering cell surface glycans: (i) identification of a target glycoconjugate 'acceptor' within cells of interest (applying the relevant probes—for example, SACK-1 mAb), (ii) use of appropriate enzymatic reagents and conditions to produce stereospecific carbohydrate substitution without compromising cell viability or producing unwanted phenotypic effects, and (iii) confirmation of target modification, as evidenced by the pertinent biochemical and functional assays, including *in vivo* demonstration of the phenotypic effect. Identification of the glycan-modified molecules is important, as

both lipids and proteins can display acceptor glycoconjugates. Under hemodynamic shear, membrane proteins are the preferred carriers of selectin ligand determinants because their extended structure yields more efficient initial contacts between flowing cells and endothelium. Our results show that glycolipids are minor carriers, and they also show that CD44 is the sole glycoprotein carrier of the sLe<sup>x</sup> determinants elicited on human MSCs by enforced fucosylation (Fig. 2b–d).

MSCs are readily obtained and culture-expanded without loss of multipotency, but their use for stem cell-based therapies is limited by poor tissue tropisms. The results presented here demonstrate that despite the absence of CXCR4 and many other effectors of homing to bone on MSCs, osteotropism can be conferred to the cells by *ex vivo* cell surface carbohydrate modification of a single glycoprotein, CD44, creating the potent E-selectin ligand HCELL. Engineered HCELL expression was enabled by rational design and development of the requisite reagents and conditions to specifically drive surface  $\alpha$ -1,3-fucosylation without detrimental effects on the cell; the resultant transient HCELL expression allows for temporal MSC homing with coincident reversion to the native CD44 glycoform soon after extravasation. By addressing the proximate obstacle in MSC-based regenerative therapeutics for systemic skeletal diseases, this technology has immediate clinical applicability. Furthermore, because E-selectin is universally displayed at sites of ischemia and inflammation in primates<sup>29,30</sup>, programmed HCELL expression should license migration and infiltration of human MSCs (and, similarly, other stem or progenitor cells) at affected tissues for regenerative therapeutics of nonskeletal conditions. Beyond the implications for tissue regeneration, our results also provide a roadmap for testing how augmented E-selectin ligand activity on other pertinent cells (for example, regulatory T cells or cytotoxic T cells) could be harnessed to promote cell migration in adoptive cell therapeutics for a variety of physiologic and pathologic processes, including immune diseases, infectious diseases and cancer, all of which are accompanied by upregulated E-selectin expression in affected endothelial beds.

## METHODS

**Human cells.** We obtained bone marrow cells from marrow bone spicules deposited on in-line filters of clinical harvests from healthy individuals (ages 21–55,  $n = 17$ ) donating marrow at the Brigham & Women's Hospital and Massachusetts General Hospital for hematopoietic stem cell transplantation. We flushed the cells from the filters and released them from bone spicules by repeated pipetting. We collected bone marrow mononuclear cells by Ficoll-Paque gradient centrifugation. We used the cells in accordance with protocols approved by the Human Experimentation and Ethics Committees of Partners Cancer Care Institutions (Boston, Massachusetts). We obtained HUVECs from a core facility at Brigham & Women's Hospital's Pathology Department and maintained them in Medium199 (Lonza Group) supplemented with 15% FBS, 5 units/ml heparin, 50  $\mu$ g/ml endothelial growth factor and 1% penicillin-streptomycin. For adhesion assays, we activated confluent monolayers of HUVECs to express E-selectin by pretreating them with 1 ng/ml interleukin-1 $\beta$  and 10 ng/ml tumor necrosis factor- $\alpha$  (both from Research Diagnostics) for 4–6 h.

**Multipotent mesenchymal stromal cell culture.** We maintained MSCs in a humidified incubator at 37 °C and 5% CO<sub>2</sub> (ref. 16). We plated bone marrow mononuclear cells at an initial density of  $2 \times 10^5$  cells/cm<sup>2</sup> in DMEM–low glucose medium supplemented with 10% FBS from selected lots. After several days, we removed nonadherent cells and harvested adherent cells by treatment with 0.05% trypsin, 0.5 mM EDTA and HBSS (Invitrogen) for <3 min at 37 °C and then replated them at a density of 50 cells/cm<sup>2</sup>. We replaced the medium at 48–72 h and every third or fourth day thereafter. We replated the cells when their density approached 40% confluence. For all experiments, we used MSCs within the first three passages and harvested them by treatment with 0.05% trypsin, 0.5 mM EDTA and HBSS for <2 min at 37 °C.

**Generation of SACK-1 monoclonal antibody.** We isolated HCELL from KG1a cells by immunoaffinity chromatography of cell lysates with mAb to CD44. We injected BALB/c mice with pure HCELL in complete Freund's adjuvant (1:1 emulsion), splitting the inoculums 50:50 between skin and intraperitoneal sites. We performed boosting 2 weeks later with pure HCELL diluted 1:1 in incomplete Freund's adjuvant and injected intraperitoneally. After 10–14 d, we boosted the immune response by intravenous injection of 5  $\mu$ g HCELL and then harvested spleens 3 d after intravenous boost. Next, we fused splenocytes with NSO myeloma cells. We screened hybridoma supernatants by flow cytometry using the hematopoietic cell lines KG1a (CD44<sup>+</sup>HCELL<sup>+</sup>HECA452<sup>+</sup>), HL60 (CD44<sup>+</sup>HCELL<sup>+</sup>HECA452<sup>+</sup>), RPMI8402 (CD44<sup>+</sup>HCELL<sup>+</sup>HECA452<sup>-</sup>), JURKAT and K562 (both are CD44<sup>+</sup>HCELL<sup>+</sup>HECA452<sup>-</sup>). We identified the SACK-1 mAb as CD44<sup>+</sup> and carbohydrate-specific by its reactivity to KG1a but not to CD44<sup>-</sup> cell lines, in conjunction with western blot evidence of its monospecificity for CD44 expressed on KG1a cells, which was sensitive to digestion with *N*-glycosidase F (New England Biolabs; digestion performed as described<sup>6,15</sup>). We determined the reactivity of SACK-1 to  $\alpha$ -2,3-sialylated glycans by treating cells with  $\alpha$ -2,3-specific sialidase from *S. pneumoniae* (Sigma).

**Recombinant expression and formulation of human  $\alpha$ -1,3-fucosyltransferase VI.** We used a *Pichia pastoris* KM 71 (arg4his4aox1:ARG4) host strain containing the gene encoding human FTVI and the N-terminal signal sequence of *Saccharomyces cerevisiae*  $\alpha$ -factor for stable expression and secretion of active FTVI into medium using online methanol sensing (sterilizable methanol sensor by Raven Biotech) and regulation of methanol addition by Alitea pumps (Alitea A.B.). After the end of fermentation, we cooled down the broth to 10 °C and the *Pichia* cells were separated by a Pellicon microfiltration system with 0.2- $\mu$ m membranes, and, subsequently, we achieved the final formulation by buffer exchange with HBSS using a Pellicon ultrafiltration system with 10-kDa ultrafiltration membranes (regenerated cellulose).

**Fucosyltransferase VI and sialidase treatment.** We treated MSCs that were either in a confluent monolayer or in suspension with 60 mU/ml FTVI in HBSS (without Ca<sup>2+</sup> or Mg<sup>2+</sup>) containing 20 mM HEPES, 0.1% human serum albumin and 1 mM GDP-fucose for 40 min at 37 °C. After incubation, we washed the MSCs with HBSS containing 0.2% BSA and 20 mM HEPES. We assessed viability routinely by trypan blue exclusion and propidium iodide staining. We then used untreated, buffer-treated (that is, without FTVI) and FTVI-treated MSCs for experiments. In some experiments, we first treated MSCs with FTVI and then subjected them to treatment with 100 mU/ml of either *Vibrio cholerae* or *S. pneumoniae* sialidase ( $\alpha$ -2,3-specific) for 1 h at 37 °C (FTVI-sialidase-MSCs). We confirmed the efficacy of sialidase treatment in each case by loss of reactivity to CSLEX1 and HECA452 as determined by flow cytometry.

**In vivo homing.** All studies were in accordance with US National Institutes of Health guidelines for care and use of animals under approval of the Institutional Animal Care and Use Committees of Massachusetts General Hospital and Harvard Medical School. We performed intravital microscopy as previously described<sup>4</sup> to analyze interactions of MSCs with mouse marrow microvascular endothelium at the parasagittal calvarium; we obtained time-sequential images after MSC injection (3  $\times$  10<sup>5</sup> cells per mouse) from individual mice. For a complete description, see **Supplementary Methods** online.

**Statistics.** We used the Student's paired *t*-test for statistical analysis; *P* values <0.05 were considered significant. Error bars represent s.e.m.

**Additional methods.** Please refer to **Supplementary Methods** for descriptions of reagents, flow cytometry, western blot analysis, immunoprecipitation studies, parallel-plate flow chamber assays, *in vivo* imaging and homing assays, and bone sectioning and immunofluorescence imaging.

*Note: Supplementary information is available on the Nature Medicine website.*

#### ACKNOWLEDGMENTS

We thank C.A. Knoblauch, L. Liu and J.Y. Lee for assistance in manuscript preparation and for skilled technical support, as well as P.V. Hauschka for helpful discussion of the data. We are grateful to the staff of the Cell Processing

Laboratory of the Bone Marrow Transplantation Unit at the Massachusetts General Hospital and the Cell Manipulation Core Facility of Dana Farber Cancer Center for their assistance in procuring the bone marrow harvest filter sets. This effort was supported by National Institutes of Health grants RO1 HL73714 (R.S.), RO1 HL60528 (R.S.) and Massachusetts General Hospital Wellman Center Advanced Microscopy startup fund (C.P.L.). This report is dedicated to the memory of Dr. Harvey R. Colten.

#### AUTHOR CONTRIBUTIONS

R.S. conceived the study and reagents, created hybridomas, developed the SACK-1 mAb and the conditions for surface fucosylation of live cells, performed experiments and supervised all research, wrote the manuscript and funded the research; J.S.M., D.W.C. and N.M.D. performed cell culture, biochemical studies and adhesion assays; J.A.S. and C.P.L. performed intravital microscopy and C.P.L. partially funded the research; R.W. synthesized fucosyltransferase.

Published online at <http://www.nature.com/naturemedicine>

Reprints and permissions information is available online at <http://npg.nature.com/reprintsandpermissions>

- Horwitz, E.M. *et al.* Isolated allogeneic bone marrow-derived mesenchymal cells engraft and stimulate growth in children with osteogenesis imperfecta: implications for cell therapy of bone. *Proc. Natl. Acad. Sci. USA* **99**, 8932–8937 (2002).
- Jin-Xiang, F., Xiaofeng, S., Jun-Chuan, Q., Yan, G. & Xue-Guang, Z. Homing efficiency and hematopoietic reconstitution of bone marrow-derived stroma cells expanded by recombinant human macrophage-colony stimulating factor *in vitro*. *Exp. Hematol.* **32**, 1204–1211 (2004).
- Gao, J., Dennis, J.E., Muzic, R.F., Lundberg, M. & Caplan, A.I. The dynamic *in vivo* distribution of bone marrow-derived mesenchymal stem cells after infusion. *Cells Tissues Organs* **169**, 12–20 (2001).
- Sipkins, D.A. *et al.* *In vivo* imaging of specialized bone marrow endothelial microdomains for tumour engraftment. *Nature* **435**, 969–973 (2005).
- Schweitzer, K.M. *et al.* Constitutive expression of E-selectin and vascular cell adhesion molecule-1 on endothelial cells of hematopoietic tissues. *Am. J. Pathol.* **148**, 165–175 (1996).
- Dimitroff, C.J., Lee, J.Y., Rafii, S., Fuhlbrigge, R.C. & Sackstein, R. CD44 is a major E-selectin ligand on human hematopoietic progenitor cells. *J. Cell Biol.* **153**, 1277–1286 (2001).
- Mauney, J.R., Volloch, V. & Kaplan, D.L. Role of adult mesenchymal stem cells in bone tissue engineering applications: current status and future prospects. *Tissue Eng.* **11**, 787–802 (2005).
- Mangi, A.A. *et al.* Mesenchymal stem cells modified with Akt prevent remodeling and restore performance of infarcted hearts. *Nat. Med.* **9**, 1195–1201 (2003).
- Pittenger, M.F. & Martin, B.J. Mesenchymal stem cells and their potential as cardiac therapeutics. *Circ. Res.* **95**, 9–20 (2004).
- Jiang, Y. *et al.* Pluripotency of mesenchymal stem cells derived from adult marrow. *Nature* **418**, 41–49 (2002).
- Sackstein, R. The lymphocyte homing receptors: gatekeepers of the multistep paradigm. *Curr. Opin. Hematol.* **12**, 444–450 (2005).
- Polley, M.J. *et al.* CD62 and endothelial cell-leukocyte adhesion molecule 1 (ELAM-1) recognize the same carbohydrate ligand, sialyl-Lewis x. *Proc. Natl. Acad. Sci. USA* **88**, 6224–6228 (1991).
- Lapidot, T., Dar, A. & Kollet, O. How do stem cells find their way home? *Blood* **106**, 1901–1910 (2005).
- Dimitroff, C.J., Lee, J.Y., Fuhlbrigge, R.C. & Sackstein, R. A distinct glycoform of CD44 is an L-selectin ligand on human hematopoietic cells. *Proc. Natl. Acad. Sci. USA* **97**, 13841–13846 (2000).
- Sackstein, R. & Dimitroff, C.J. A hematopoietic cell L-selectin ligand that is distinct from PSGL-1 and displays *N*-glycan-dependent binding activity. *Blood* **96**, 2765–2774 (2000).
- Pittenger, M.F. *et al.* Multilineage potential of adult human mesenchymal stem cells. *Science* **284**, 143–147 (1999).
- Kobzdej, M.M., Leppanen, A., Ramachandran, V., Cummings, R.D. & McEver, R.P. Discordant expression of selectin ligands and sialyl Lewis x-related epitopes on murine myeloid cells. *Blood* **100**, 4485–4494 (2002).
- Xia, L., McDaniel, J.M., Yago, T., Doeden, A. & McEver, R.P. Surface fucosylation of human cord blood cells augments binding to P-selectin and E-selectin and enhances engraftment in bone marrow. *Blood* **104**, 3091–3096 (2004).
- Hidalgo, A. & Frenette, P.S. Enforced fucosylation of neonatal CD34<sup>+</sup> cells generates selectin ligands that enhance the initial interactions with microvessels but not homing to bone marrow. *Blood* **105**, 567–575 (2005).
- Murray, B.W., Takayama, S., Schultz, J. & Wong, C.H. Mechanism and specificity of human  $\alpha$ -1,3-fucosyltransferase V. *Biochemistry* **35**, 11183–11195 (1996).
- Schranz, N. *et al.* Manganese induces apoptosis of human B cells: caspase-dependent cell death blocked by bcl-2. *Cell Death Differ.* **6**, 445–453 (1999).
- de Bruyn, K.M., Rangarajan, S., Reedquist, K.A., Figdor, C.G. & Bos, J.L. The small GTPase Rap1 is required for Mn<sup>2+</sup>- and antibody-induced LFA-1- and VLA-4-mediated cell adhesion. *J. Biol. Chem.* **277**, 29468–29476 (2002).
- Alon, R. *et al.* The integrin VLA-4 supports tethering and rolling in flow on VCAM-1. *J. Cell Biol.* **128**, 1243–1253 (1995).

24. Chigaev, A. *et al.* Real time analysis of the affinity regulation of  $\alpha_4$ -integrin. The physiologically activated receptor is intermediate in affinity between resting and  $Mn^{2+}$  or antibody activation. *J. Biol. Chem.* **276**, 48670–48678 (2001).
25. Takamatsu, Y., Simmons, P.J. & Levesque, J.P. Dual control by divalent cations and mitogenic cytokines of  $\alpha_4\beta_1$  and  $\alpha_5\beta_1$  integrin avidity expressed by human hemopoietic cells. *Cell Adhes. Commun.* **5**, 349–366 (1998).
26. Mazo, I.B., Quackenbush, E.J., Lowe, J.B. & von Andrian, U.H. Total body irradiation causes profound changes in endothelial traffic molecules for hematopoietic progenitor cell recruitment to bone marrow. *Blood* **99**, 4182–4191 (2002).
27. Mohler, W., Millard, A.C. & Campagnola, P.J. Second harmonic generation imaging of endogenous structural proteins. *Methods* **29**, 97–109 (2003).
28. Hauschka, P.V., Lian, J.B. & Gallop, P.M. Direct identification of the calcium-binding amino acid, gamma-carboxyglutamate, in mineralized tissue. *Proc. Natl. Acad. Sci. USA* **72**, 3925–3929 (1975).
29. Yao, L. *et al.* Divergent inducible expression of P-selectin and E-selectin in mice and primates. *Blood* **94**, 3820–3828 (1999).
30. Mocco, J. *et al.* HuEP5C7 as a humanized monoclonal anti-E/P-selectin neurovascular protective strategy in a blinded placebo-controlled trial of nonhuman primate stroke. *Circ. Res.* **91**, 907–914 (2002).